Modeling Drug Release of Phosphoramidate-based Antibody-drug Conjugates using Machine Learning Metadynamics

Rizka Nur Fadilla and Yoshitada Morikawa
大阪大学 大学院工学研究科

1. Introduction

Antibody-drug conjugates (ADCs) are a type of biopharmaceutical drug designed to deliver cytotoxic payloads (chemotherapy drugs) specifically to cancer cells. The goal is to kill cancer cells while minimizing harm to healthy cells, a common challenge in conventional cancer chemotherapy. The goal is achieved by linking the payload to an antibody that can precisely locate cancer cells via a suitable linker. The success of ADCs depends on the antibody's specificity, the linker's cleavage selectivity (remaining intact outside but readily cleaved inside cancer cells), and the potency of the payload [1].

One of the most critical challenges in ADC development is the instability of the linker. This issue can lead to the premature release of the payload, for instance, in the bloodstream, before it reaches the targeted cancer cells. Such premature release can cause toxicities, as demonstrated by the withdrawal of Mylotarg from the market in 2010 [3], after its FDA approval in 2000. Understanding and overcoming these challenges is crucial for the successful development of ADCs.

The phosphoramidate-based linker (see Fig. 1) is one of several proposed linkers that potentially tackle the linker instability challenge. It exhibits stability at neutral pH (representing the environment outside cancer cells), with a controllable rapid release in low pH (representing the environment inside cancer cells). The linker has shown its potency in carrying a diverse payload, which could significantly enhance the efficacy of ADCs [4-6]. Despite these encouraging results, no approved ADC utilizing this linker has been reported yet. One possible explanation is the lack of a clear mechanistic understanding of how the payload release is controlled.

Exploring the potential energy surface (PES) of the involved chemical reactions is essential to gaining insight into the payload release mechanism from a phosphoramidate-based linker. This PES can be represented using an interatomic potential model. Achieving an accurate representation of the PES involves solving the Schrödinger equation, which can be approximated through density-functional theory (DFT). However, the high computational cost of DFT often limits its use for statistical sampling, such as in metadynamics simulations [7].

Recently, machine learning techniques have shown promise in accurately representing the PES when trained with data generated from DFT-based calculations. Here, we have developed a machine learning interatomic potential for phosphoramidate in aqueous

solution. Subsequently, we utilized this developed potential to explore the PES associated with the payload release from a phosphoramidate-based linker.

2. Computational Method

2.1 Deep Potential

We utilize the Deep Potential (DP) scheme [8] to develop a machine learning interatomic potential. Within the DP scheme, the potential energy of atomic configurations is represented as the sum of atomic energies. The local environment of the atom within a specified cutoff radius determines each atomic energy. The process begins by establishing the local coordinate information of each atom while preserving translational, rotational, and permutational symmetries. Subsequently, this local coordinate information is used as input for a deep neural network, generating atomic energies as the output. The DP scheme implementation is carried out using the DeePMD-kit [9].

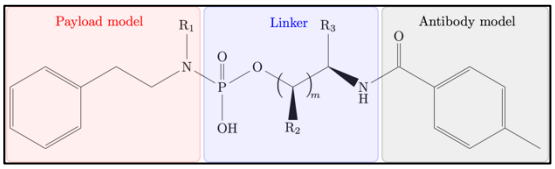

Fig. 1: Components of antibody-drug conjugates with phosphoramidate-based linker. Symbols R_1, R_2, and R_3 denote the substituent of the linker.

2.2 Density-functional Theory (DFT)

Density-functional theory (DFT) is a computational method based on quantum mechanics that accurately investigates the electronic structure of atoms, molecules, and solids. This study employs DFT to generate training data for input into the DP network. We utilized the CP2K software [10] to calculate the system's energy and atomic forces. The training data comprises two systems: pure bulk water and the phosphoramidate in aqueous solution. Fig. 2 and 3 illustrate the typical training structures used in this context.

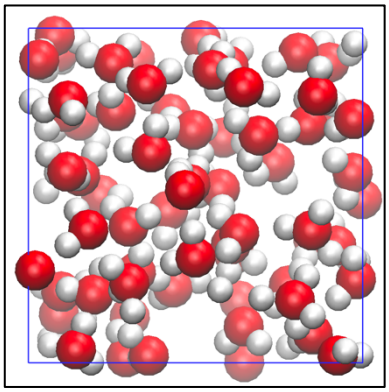

Fig. 2: Pure bulk water. The red and white colors denote oxygen and hydrogen atoms, respectively.

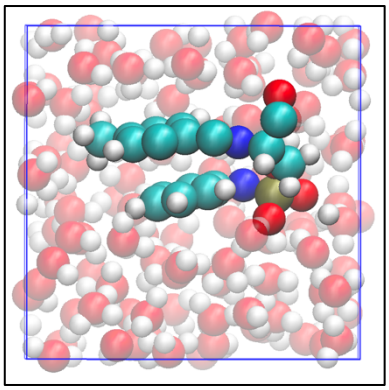

Fig. 3: Phosphoramidate-based ADC in aqueous solution. The red, white, green, blue, and brass colors denote oxygen, hydrogen, carbon, nitrogen, and phosphor atoms.

2.3 Metadynamics

Metadynamics is a simulation technique employed to investigate the PES and accelerate the sampling of rare events by periodically introducing bias potential. This bias potential is incorporated into the

space of selected collective variables (CVs) that characterize the chemical reaction. In our study, we have chosen two CVs: the P-N coordination number (reflecting the P-N bond cleavage) and the P-O coordination number (representing the P-O bond formation). To conduct the metadynamics simulation, we utilized Plumed [11] patched with LAMMPS [12].

3. Validation of Deep Potential

To validate the accuracy of the developed potential, we compare the machine learning (ML) potential's prediction on energy and atomic forces to the DFT results (Section 3.1). We also calculate both quantities' root mean square errors (RMSE). We further use the ML potential to simulate the behavior of liquid water and compute the oxygen-oxygen radial distribution function (Section 3.2).

3.1 DFT vs Deep Potential

Parity plots of the energy and atomic forces, DFT vs ML, over 805 test data, are shown in Fig. 4. The test data are not included in the training process. They consist of pure bulk water and phosphoramidate in aqueous solution. The RMSE of energy and atomic forces are smaller than one meV/atom and 100 meV/Å, which indicates a good quality of potential.

3.2 Radial Distribution Function

The performance of ML potential is further validated through the oxygen-oxygen radial distribution function (RDF) of pure bulk water, as shown in Fig. 5. The discrepancy between the predicted RDF and the experimental one is not significant. The ML potential predicted the water molecules to be slightly more localized than the experimental results. This result and the parity plot indicate that the ML potential is reasonably good.

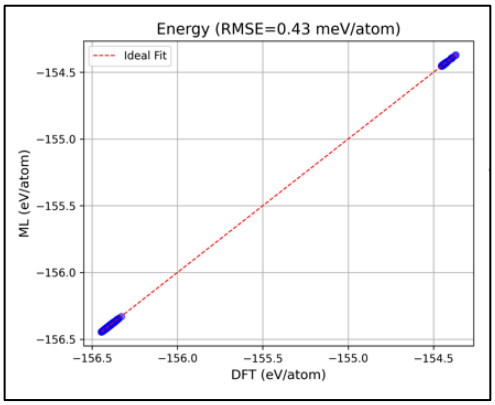

(a)

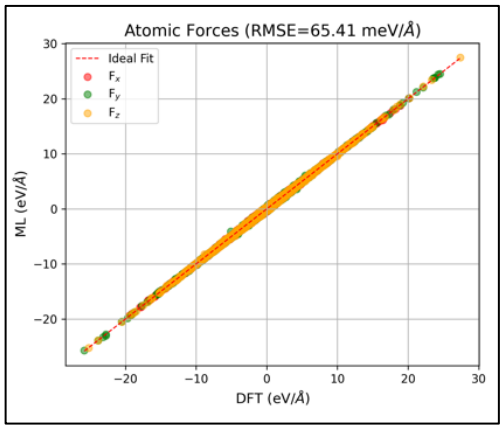

(b)

Fig. 4: Parity plot of (a) energy and (b) atomic forces.

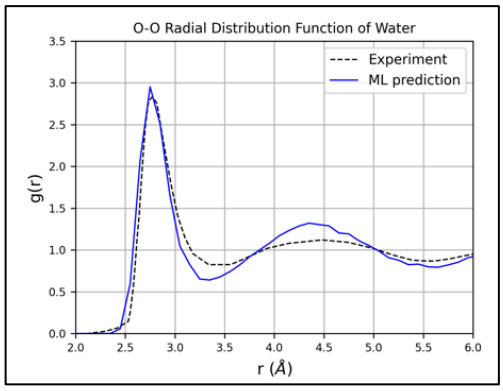

Fig. 5: Oxygen-oxygen radial distribution function of water.

4. Tautomerization

ML metadynamics is performed to simulate the payload release for clarifying the

detailed mechanism. Prior to payload release, we observed tautomerization occurred in the simulation. The tautomerization changes the molecule from having single nitrogen-protonated to double nitrogen-protonated, as shown in Fig. 6 (a) and (b), respectively. ML metadynamics simulation is performed to simulate the payload release to clarify the detail mechanism. Prior to payload release, we observed tautomerization in the simulation. The tautomerization changes the molecule from having one hydrogen bonded to nitrogen to two hydrogen, as shown in Fig. 6. Further simulation and analysis to clarify the reaction mechanism are ongoing.

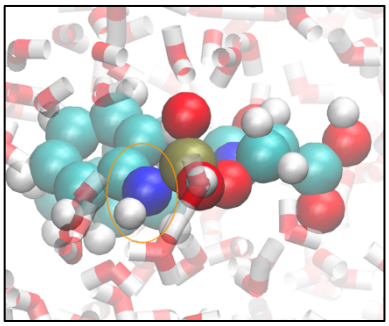

(a)

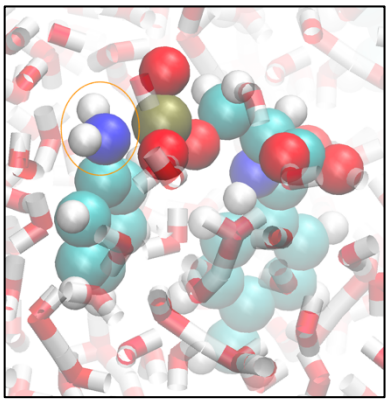

(b)

Fig. 6: (a) Initial and (b) final state of tautomerization.

5. Conclusion

We have developed a machine learning potential using the Deep Potential scheme, which can represent the interatomic interactions of phosphoramidate in aqueous solution. When coupled with metadynamics simulation, this machine learning potential emerges as a promising tool for exploring the potential energy surface, especially in the presence of rare events. Once this work is completed, we expect to be able to clarify the payload release mechanism in detail.

Bibliography

(1) R. V. J. Chari, et al., Angewandte Reviews, **53**, 3751-4005 (2014).

(2) A. Samantasinghar, et al., Biomedicine & Pharmacotherapy, 113308 (2023).

(3) A. D. Ricart, Clinical Cancer Research, **17**, 6417-6472 (2011).

(4) C. J. Choy, et al., Bioconjugate Chemistry, **27**, 824-830 (2016).

(5) C. J. Choy, et al., Bioconjugate Chemistry, **27**, 2206-2213 (2016).

(6) F. P. Olatunji, et al., Bioconjugate Chemistry, **32**, 2386-2396 (2021).

(7) A. Barducci, et al., Wiley Interdisciplinary Reviews: Computational Molecular Science, **1**, 826-843 (2011).

(8) L. Zhang, et al., Physical Review Letters, **120**, 143001 (2018).

(9) H. Wang, et al., Computer Physics Communications, **228**, 178-184 (2018).

(10) T. Kühne, et al., Journal of Chemical Physics, **152**, 194103 (2020).

(11) G. A. Tiberllo, et al., Computer Physics Communications, **185**, 604 (2014).

(12) A. P. Thompson, et al., Computer Physics Communications, **271**, 10817 (2022).